

Terahertz emission by plasma waves in 60 nm gate high electron mobility transistors

W. Knap and J. Lusakowski^{a)}

GES, CNRS-Université Montpellier 2, 34900 Montpellier, France and Electrical, Computer and System Engineering Department, Rensselaer Polytechnic Institute, Troy, New York 12180

T. Parenty, S. Bollaert, and A. Cappy

EMN-DHS UMR CNRS 8520, Avenue Poincaré, 59652 Villeneuve d'Ascq, France

V. V. Popov

Institute of Radioengineering and Electronics, Russian Academy of Sciences, 410019 Saratov, Russia

M. S. Shur

Center for Broadband Data Transport and Electrical, Computer and System Engineering Department, Rensselaer Polytechnic Institute, Troy, New York 12180

(Received 4 August 2003; accepted 2 February 2004)

We report on the resonant, voltage tunable emission of terahertz radiation (0.4–1.0 THz) from a gated two-dimensional electron gas in a 60 nm InGaAs high electron mobility transistor. The emission is interpreted as resulting from a current driven plasma instability leading to oscillations in the transistor channel (Dyakonov–Shur instability). © 2004 American Institute of Physics.

[DOI: 10.1063/1.1689401]

Plasma waves in a gated two-dimensional electron gas have a linear dispersion law, similar to that of sound waves. The transistor channel acts as a resonator cavity for plasma waves that can reach THz frequencies for a sufficiently short (nanometer-sized) field effect transistor.¹ As was predicted in Ref. 2, when a current flows through a field effect transistor, the steady state can become unstable against the generation of plasma waves (Dyakonov–Shur instability) leading to the emission of an electromagnetic radiation at plasma wave frequencies. The emission is predicted to have thresholdlike behavior. It is expected to appear abruptly after the device current exceeds a certain threshold value for which the increment of the plasma wave amplitude exceeds losses related to electron collisions with impurities and/or lattice vibrations.

The excitation of plasma waves in a field effect transistor channel can be also used for the detection of terahertz radiation.³ Recent reports demonstrated a resonant⁴ detection in GaAs-based high electron mobility transistors (HEMTs) and in gated double quantum well heterostructures.⁵

This is the first report of resonant THz emission by plasma generation. The terahertz emission (0.4–1.0 THz) was obtained by using an InGaAs HEMT with a 60-nm-long gate. We show that the results can be interpreted assuming that the emission is caused by the current driven plasma instability leading to terahertz oscillations in the channel through Dyakonov–Shur instability.

Lattice-matched InGaAs/AlInAs HEMTs grown by molecular beam epitaxy on an InP substrate were used in this study. The active layers consisted of a 200 nm In_{0.52}Al_{0.48}As buffer, a 20 nm In_{0.53}Ga_{0.47}As channel, a 5-nm-thick undoped In_{0.52}Al_{0.48}As spacer, a silicon planar doping layer of

$5 \times 10^{12} \text{ cm}^{-2}$, a 12-nm-thick In_{0.52}Al_{0.48}As barrier layer, and, finally, a 10-nm-silicon-doped In_{0.53}Ga_{0.47}As cap layer. Details of the technological process are given elsewhere.⁶ The gate length was 60 nm, and the drain-source separation was 1.3 μm . An InP-based HEMT was chosen for its high InGaAs channel mobility and high sheet carrier density.

Output and transfer characteristics are shown in Fig. 1. The low field, linear output region is marked by the dotted line. The deviation of the $I_d(U_{sd})$ curve from linear behavior indicates the beginning of the saturation region. The arrow indicates the emission threshold voltage, $U_{sd} \sim 200 \text{ mV}$ at $I_d \sim 4.5 \text{ mA}$. The horizontal dashed line shows the level of the current saturation ($I_d \sim 4.8 \text{ mA}$). The $I_d(U_{sd})$ characteristic shows an unstable behavior for U_{sd} higher than 300 mV. This well-known phenomenon is related to a self-excitation

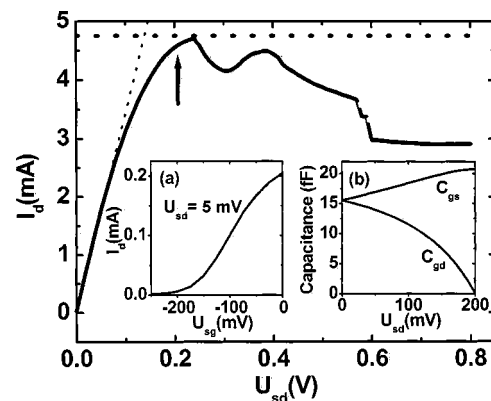


FIG. 1. Output characteristic (drain current I_d vs source-drain voltage U_{sd}). The arrow marks the emission threshold voltage, $U_{sd} \sim 200 \text{ mV}$. The horizontal dashed line shows the saturation current of 4.8 mA, used in the calculation. The slope of the low voltage linear behavior is marked by the dotted line. (a) Transfer characteristic (I_d vs source-gate voltage U_{sg} for $U_{sd} = 5 \text{ mV}$). (b) Calculated source-gate (C_{sg}) and gate-drain (C_{gd}) capacitance vs U_{sd} . The saturation voltage was assumed to be 200 mV.

^{a)}Also at: Institute of Experimental Physics, University of Warsaw, Hoza 69, 00-681 Warsaw, Poland; electronic mail: knap@univ-montp2.fr

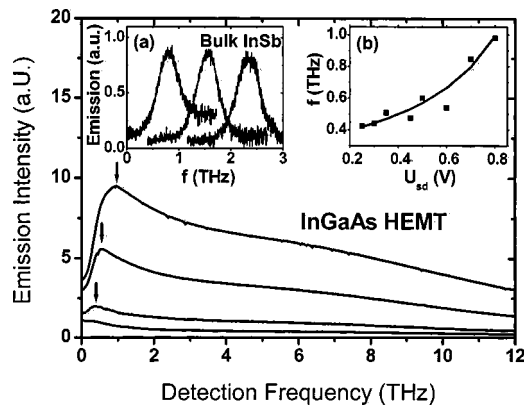


FIG. 2. Spectra of emission from an InGaAs HEMT for different source-drain voltages, U_{sd} . The arrows mark emission maxima at 0.42, 0.56, and 1.0 THz for U_{sd} equal to 0.3, 0.6, and 0.8 V, respectively. (a) Cyclotron emission from a bulk InSb emitter analyzed by an InSb detector (detector calibration procedure). Different curves correspond to different values of the emitter magnetic field: 0.4, 0.8, and 1.2 T (from left to right). (b) Resonant frequency of the emission f from an InGaAs HEMT vs U_{sd} .

of the transistor at relatively low frequencies. The transistor threshold voltage, $U_{th} \sim 200$ mV, is determined from the transfer characteristic [see Fig. 1(a)].

One of the main experimental difficulties lies in achieving the resonant cavity boundary conditions required for the development of plasma instability upon successive reflections of plasma waves from the channel borders.¹ Ideally, the required boundary conditions are gate-source impedance at the source side of the channel equal to zero and gate-drain impedance at the drain side tending to infinity. In the present work, boundary conditions close to the ideal ones were achieved by short circuiting the gate with the source and driving the transistor into the saturation region. Figure 1(b) shows results of capacitance calculations for our device using the model of Ref. 7. One can see that the gate-source capacitance increases and the gate-drain capacitance approaches zero (in an ideal case) when the drain bias approaches the saturation region.

The emission experiments were performed in the cyclotron emission spectrometer⁸ used earlier for investigations of weak THz cyclotron resonance emission in GaAs/AlGaAs heterojunctions. In this spectrometer, the terahertz source and detector under study are placed in a copper waveguide cooled to 4.2 K and completely isolated from 300 K background radiation. The emitted radiation is analyzed by a magnetically tunable InSb cyclotron detector calibrated with InSb and GaAs bulk emitters. The emission frequency can be tuned by the magnetic field in a wide range from subTHz up to a few THz. A few emission spectra from a bulk InSb cyclotron resonance emitter obtained during the calibration procedure are shown in Fig. 2(a). After calibration of the detector, the bulk emitter was replaced by the HEMT. Voltage pulses were applied between drain and source, and a standard lock-in technique was used.

A few measured spectra are shown in Fig. 2. The spectra exhibit one main emission line. The peak emission frequency shifts from ~ 0.42 up to ~ 1 THz with increasing the source-drain voltage [see Fig. 2(b)]. No emission was observed until the drain current (drain voltage) reached a certain threshold ~ 4.5 mA (~ 200 mV). Above the threshold, a strong emis-

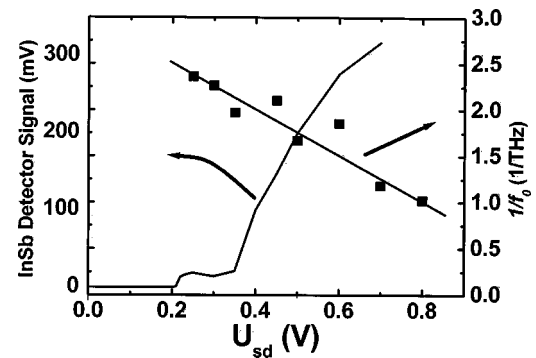


FIG. 3. Amplitude of the resonant emission signal vs source-drain voltage (left vertical axis). Inverse frequency ($1/f_0$) vs source-drain voltage (right vertical axis). The straight line represents the best linear fit of Eq. 2.

sion signal (sharply increasing with the bias) was observed. The threshold behavior can be clearly seen in Fig. 3 showing the resonant line emission intensity vs source-drain voltage.

The observed radiation power was in the nW range as compared to the pW power of the bulk InSb emitters used for calibration. The total power corresponds to the power density of several W/cm², at least 6 orders of magnitude higher than the total integrated intensity of the black body radiation at room temperature in the THz range.

The resonant frequency of the emission is determined by the sheet electron density under the gate, the electron drift velocity, and the effective gate length L_{eff} . The last depends on the geometry of the device but, in the saturation regime, is also affected by the drain voltage due the gate length modulation effect. The effective gate length at zero source-drain bias, $L_{eff} = L + 2d$, where L is the geometric gate length and d is the thickness of the wide band barrier layer (for our device, $d = 17$ nm and $L_{eff} = 94$ nm).

According to Refs. 1 and 2, the frequency of the lowest fundamental plasma mode f_0 excited in the gated region of the device is given by

$$f_0 = \frac{(s^2 - v_o^2)}{4sL_{eff}}, \quad s = \sqrt{\frac{eU_0}{m}}, \quad (1)$$

where v_o is the electron drift velocity in the channel, s is the plasma wave velocity, e is the electron charge, m is the effective electron mass ($m \sim 0.042 m_o$, where m_o is the free electron mass) and U_0 is the effective gate-to-channel voltage swing. The swing voltage can be estimated from the I(V) characteristics to be $U_0 = (80 \pm 30)$ mV.⁹ We assumed a relatively big error bar on the swing voltage to account for a nonuniformity of the electron sheet density in the channel. The effective electron sheet density in the channel, $n_s = \epsilon \epsilon_o U_0 / (ed)$, is approximately equal to $(3.3 \pm 1.2) \times 10^{11}$ cm⁻² for our device ($\epsilon = 12.7$) and the plasma wave velocity $s = (5.8 \pm 1.2) \times 10^5$ m/s. In the absence of current (when the electron drift velocity $v_o = 0$), Eq. (1) gives the resonant frequency $f_0 = (1.6 \pm 0.3)$ THz. This value is reduced when a current flows through the device. Using Eq. (1) and the value of s estimated above, we calculated the drift velocity v_o necessary to reach the experimentally observed frequency of 0.42 THz and obtained $v_o = (4.9 \pm 1.2) \times 10^5$ m/s. This value is in very good agreement with recent Monte Carlo calculations of the drift velocity for nanometer InGaAs HEMTs.^{10,11}

The observed line is nonsymmetric with a long high frequency tail. This high frequency part of the emission spectrum can be explained as resulting from the excitation of higher order and/or oblique modes in the gated region of the device. It can be also due to the plasma wave excitations in the ungated regions of the transistor channel.¹²

As the drain bias increases, the gate length modulation effect decreases the effective channel length (see, for example, Ref. 13). Gate length modulation takes place since, in the saturation region, the channel splits into two parts—an effective field effect transistor section and a high field region; the latter being formed at the drain side of the channel and spreads toward the source with an increase of the applied source-drain voltage. The decrease of the effective length of the channel can be described by a phenomenological formula

$$L_{\text{eff}}(U_{\text{ds}}) = L_{\text{eff}}(0) - \frac{U_{\text{ds}} - U_{\text{sat}}}{E_d}, \quad (2)$$

where U_{sat} is the source-drain saturation voltage and E_d is the effective electric field. As a consequence, we expect $1/f_o$ to be a linear function of $U_{\text{ds}} - U_{\text{sat}}$. Figure 3 shows that $(1/f_o)$ can indeed be approximated by a straight line as predicted by this simple model. We determined the effective electric field in the high field region to be $E_d = 4 \times 10^4$ V/cm, while the saturation voltage was taken as $U_{\text{sat}} = 240$ mV, the voltage for which the first well resolved resonant emission ($f_o = 0.42$ THz) was observed.

In summary, we report on a resonant THz emission from an InGaAs HEMT with a 60 nm gate length and interpret it as caused by the Dyakonov–Shur instability of plasma waves in the gated two-dimensional electron system. We show that: (i) the observed emission appears once the device current exceeds a certain threshold, (ii) by driving the transistor into the saturation region one reaches required boundary conditions, and (iii) the value of the resonant frequency and the range of its tunability agree with theoretical predictions.

The authors would like to thank Professor M. Dyakonov for his constant interest in this work and for many important and useful discussions. The authors gratefully acknowledge support from the CNRS program New THz Emitters and Detectors, Region Languedoc Roussillon, the French Minis-

try of Research and New Technologies program ACI Nanosciences and Nanotechnologies, and DARPA (Dr. Edgar Martinez and Dr. Dwight Woolard, project monitors). V.V.P. acknowledges support from the Russian Foundation for Basic Research (Grant No. 03-02-17219).

¹M. Dyakonov and M. S. Shur in *Terahertz Sources and Systems*, edited by R. E. Miles (Kluwer, Netherlands, 2001), pp. 187–207.

²M. Dyakonov and M. S. Shur, *Phys. Rev. Lett.* **71**, 2465 (1993).

³M. Dyakonov and M. S. Shur, *IEEE Trans. Electron Devices* **43**, 380 (1996).

⁴W. Knap, Y. Deng, S. Romyantsev, and M. S. Shur, *Appl. Phys. Lett.* **81**, 4637 (2002).

⁵X. G. Peralta, S. J. Allen, and M. C. Wankee, *Appl. Phys. Lett.* **81**, 1627 (2002).

⁶T. Parenty, S. Bollaert, J. Mateos, X. Wallart, and A. Cappy, in *Proc. of Indium Phosphide and Related Material (IPRM) Conference*, (Nara, Japan, 2001), pp. 626–629.

⁷T. Fjeldly, T. Ytterdal, and M. S. Shur, *Introduction to Device and Circuit Modeling for VLSI* (Wiley, New York, 1998), p. 303.

⁸W. Knap, *Rev. Sci. Instrum.* **63**, 3293 (1992).

⁹The effective swing voltage U_o , can be estimated from the formula $U_o \sim U_{\text{gs}} - U_{\text{th}} - (I_d R_s / 2) - (U_{\text{ch}} / 2)$ where U_{gs} is the external voltage swing ($U_{\text{gs}} = 0$ in our case), $U_{\text{th}} = -200$ mV is the threshold voltage [see Fig. 1 (a)], I_d is the drain current, R_s is the total source series resistance, and U_{ch} is the voltage drop on the gated part of the channel. The total source-drain voltage can be written as $U_{\text{sd}} = U_{\text{ch}} + I_d R_s$. Since $L_{\text{eff}} \ll L_{\text{sd}}$, where $L_{\text{sd}} = 1.3 \mu\text{m}$ is the drain-source separation, most of the source-drain voltage drop in the linear region occurs across (R_s) determined by the source-gate and drain-gate access regions. Therefore, U_{ch} can be neglected and $R_s = 29 \Omega$ can be determined from the slope of the output characteristic (the dotted line in Fig. 1). We observed well resolved resonant emission ($f_o = 0.42$ THz) for $U_{\text{sd}} = 240$ mV. Hence, for a saturation current $I_d = 4.8$ mA we obtain $I_d R_s = 140$ mV and $U_{\text{ch}} = 100$ mV. Therefore, the swing voltage can be estimated as $U_o = 80$ mV.

¹⁰Y. Yamashita, A. Endoh, K. Shinohara, T. Matsui, S. Hiyamizu, and T. Timura, *IEEE Electron Device Lett.* **23**, 573 (2002).

¹¹A simple estimation of the order of magnitude of the drift velocity for our device can be obtained as $v_{\text{eff}} = I_{\text{ds}} / (en_s W)$. For $W = 50 \mu\text{m}$, $I_{\text{ds}} = 4.8$ mA, and the carrier density $3.3 \times 10^{11} / \text{cm}^2$ one obtains $v_{\text{eff}} = 2 \times 10^5$ m/s. The value of v_o in Eq. (3) may differ from v_{eff} since the velocity distribution in the channel is not uniform in the saturation regime, where the measurements were performed, but these values should be of the same order of magnitude.

¹²A. Satou, I. Khmyrova, V. Ryzhii, and M. S. Shur, *Semicond. Sci. Technol.* **18**, 460 (2003).

¹³K. Lee, M. S. Shur, T. A. Fjeldly, and T. Ytterdal, *Semiconductor Device Modeling for VLSI* (Prentice Hall, Englewood Cliffs, NJ, 1993), pp. 340–358.